

See discussions, stats, and author profiles for this publication at:
<https://www.researchgate.net/publication/222393393>

Electronic structure of indium phosphide clusters: Anion photoelectron spectroscopy of In_xP_x^- and $\text{In}_{x+1}\text{P}_x^-$ ($x=1-13$) clusters

ARTICLE in CHEMICAL PHYSICS LETTERS · JULY 1999

Impact Factor: 1.9 · DOI: 10.1016/S0009-2614(99)00671-5

CITATIONS

45

READS

15

3 AUTHORS, INCLUDING:



[Knut R Asmis](#)

University of Leipzig

103 PUBLICATIONS 2,461 CITATIONS

SEE PROFILE



[Travis Taylor](#)

Lam Research Corporation

29 PUBLICATIONS 1,009 CITATIONS

SEE PROFILE

Electronic structure of indium phosphide clusters: anion photoelectron spectroscopy of In_xP_x^- and $\text{In}_{x+1}\text{P}_x^-$ ($x = 1-13$) clusters

Knut R. Asmis, Travis R. Taylor, Daniel M. Neumark *

Department of Chemistry, University of California, Berkeley, CA 94720, USA
Chemical Sciences Division, Lawrence Berkeley National Laboratory, Berkeley, CA 94720, USA

Received 13 April 1999; in final form 11 June 1999

Abstract

Photoelectron spectra for indium phosphide (InP) cluster anions comprised of up to 27 atoms were measured at a photodetachment wavelength of 266 nm. Results are presented for cluster anions of both stoichiometric and non-stoichiometric composition (In_xP_x^- , $\text{In}_{x+1}\text{P}_x^-$; $x = 1-13$). In_3P_3 exhibits the lowest electron affinity (EA) of all the clusters studied, indicating a particularly stable neutral species. The EAs of the stoichiometric clusters are considerably lower than those of the corresponding non-stoichiometric clusters, suggesting the presence of closed-shell ground states for the neutral In_xP_x clusters. Remarkable agreement between the experimental EAs and those derived from calculations on quantum dots is found. © 1999 Elsevier Science B.V. All rights reserved.

1. Introduction

Indium phosphide (InP) based materials have become an important class of III–V semiconductors, because of their application in electronic and photonic devices used for example in high-quality fiber-optics communication systems [1]. The successful synthesis of colloidal dispersions of quantum dots of crystalline InP with narrow size distributions [2] has led to experimental [3,4] and theoretical [5,6] characterization of these quantum confined InP systems. The synthesized clusters contain ~ 700–9000 atoms and behave like perturbed bulk-like species. These

results suggest it would be of interest to study InP clusters in the 10–200 atom size regime, since this is where the most dramatic evolution from molecular to bulk-like properties might be expected to occur. However, little experimental information is available for clusters in this size range.

Anion photoelectron spectroscopy is a particularly useful technique to study semiconductor clusters, since the use of anionic precursors enables one to study the electronic structure of clusters mass-selectively. It has been applied successfully to the study of pure elemental [7–11] and, to a lesser extent, binary [12–17] semiconductor clusters. Photodetachment studies on InP cluster anions are limited to two previous studies. Xu et al. [18] reported photoelectron spectra for small indium phosphide cluster anions (In_xP_y^- ; $x, y = 1-4$). They observed a con-

* Corresponding author. Fax: +1 510 642 6262; e-mail: dan@radon.cchem.berkeley.edu

siderable gap for all even clusters between the bands corresponding to transitions to the ground and the first excited states of the neutral. Higher-resolution zero electron kinetic energy (ZEKE) photodetachment studies were performed on In_2P^- and InP_2^- [19]. Prior to the photodetachment work, Mandich and co-workers [20,21] used photodissociation followed by photoionization mass spectrometry to measure near-IR and visible absorption spectra (from 0.65 to 2.0 eV) for InP neutral clusters containing 5–14 atoms, including the stoichiometric clusters In_xP_x ($x = 3\text{--}7$). They observed a higher absorption onset for the even clusters, consistent with the anion photodetachment studies. Remarkably, the onset for the even clusters was close to the band gap for bulk crystalline InP.

In the present Letter we report the photoelectron spectra of InP cluster anions containing up to 27 atoms (In_xP_x^- , $\text{In}_{x+1}\text{P}_x^-$; $x = 1\text{--}13$). We discuss the evolution of the electronic structure in general and the cluster electron affinity (EA) in particular as a function of cluster size. The present study can be seen as a continuation of the systematic study of mixed III–V clusters in our group, which so far has covered clusters of InP, GaP, and BN [17–19,22–24].

2. Experimental

The negative ion time-of-flight (TOF) photoelectron spectrometer used in this study has been described previously [25,26], with exception of a shorter electron flight tube, which was installed to increase the acceptance angle of the electron detector. Indium phosphide clusters are prepared by laser vaporization with the second harmonic (532 nm, 7.5 mJ/per pulse) of a Nd:YAG laser tightly focussed onto a rotating and translating indium phosphide disc. The resulting plasma is entrained in a pulse of Ar carrier gas from a piezoelectric valve. The plasma is expanded through a clustering channel. Ions formed in the expansion are extracted perpendicularly to the expansion by means of a pulsed electric field and accelerated to a beam energy of 3.75 keV. The extracted ions enter a linear reflectron TOF mass spectrometer, where they separate in time and space according to their mass-to-charge ratios. The mass

resolution is $m/\Delta m \approx 2000$. Photoelectrons are detached from the mass-selected ions by a fixed frequency laser pulse from a second Nd:YAG laser. The laser firing delay is varied until optimal temporal overlap is achieved with the ion of interest. The fourth harmonic (266 nm, 4.657 eV) of the Nd:YAG laser with a typical laser fluence of 7 mJ/cm² was used in the present study. The instrument is operated at 20 Hz. The angle between the laser polarization and the direction of electron collection can be varied by means of a half-wave plate. All spectra reported here were measured at a laser polarization angle of $\theta = 55^\circ$ (magic angle).

The photoelectron kinetic energy is determined by time-of-flight. The detached electrons are detected at the end of a 30 cm magnetically shielded flight tube, mounted orthogonal to the laser and ion beam. The electron detector subtends a solid angle of 0.01 sr, i.e., 0.1% of the detached photoelectrons are detected. With the shorter flight tube, the instrumental resolution is ~ 30 meV for an electron kinetic energy (eKE) of 0.65 eV and degrades as $(\text{eKE})^{3/2}$. Ultraviolet photons efficiently eject electrons from metal surfaces, resulting in a residual background photoelectron contribution of typically 1 electron per 10 laser shots at 266 nm, primarily at low eKE. Background spectra were recorded on a daily basis, summed and then subtracted from the acquired data.

3. Results

A mass spectrum of the larger indium phosphide cluster anions generated in our laser ablation source is shown in Fig. 1. A wide variety of clusters are generated that can be grouped into cluster series differing by one InP unit. The series In_xP_x^- and $\text{In}_{x+1}\text{P}_x^-$ are marked. Within each series the intensity distribution of neighboring clusters is smooth, i.e., no obvious intensity discontinuities (magic numbers) are observed. The formation of indium-rich clusters is favored under the experimental conditions used here. An excerpt of the mass spectrum is shown with larger magnification in the top right-hand corner of Fig. 1. It shows that each band associated with a cluster anion of particular stoichiometry consists of a series of peaks, reflecting the natural isotope distri-

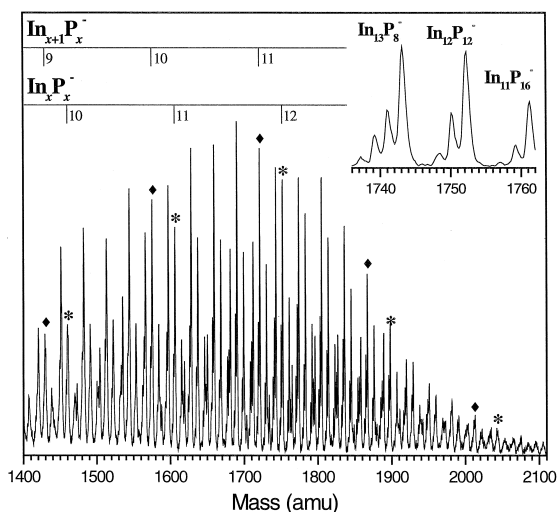


Fig. 1. Mass spectrum of larger indium phosphide clusters anions. Clusters of type In_xP_x^- (asterisks) and $\text{In}_{x+1}\text{P}_x^-$ (diamonds) are marked. An excerpt of this spectrum is shown with larger magnification in the top right-hand corner.

bution of indium atoms (96% ^{115}In , 4% ^{113}In) in the source disc. This spectrum demonstrates that in the cluster size regime we are probing (< 2100 AMU), complete mass-separation of the cluster anions of interest is obtained.

The 266 nm photoelectron spectra of the indium phosphide cluster anions In_xP_x^- and $\text{In}_{x+1}\text{P}_x^-$ ($x = 1-13$) are shown in Figs. 2 and 3. The spectra show partially resolved electronic bands, with the number of distinct bands decreasing for the larger clusters. The vertical detachment energies (VDEs) for selected bands, marked with a dot in Figs. 2 and 3, and estimated electron affinities (EAs), indicated by an arrow, are listed in Table 1. The determination of the VDEs is straightforward, as each corresponds to a band maximum, while that of the EA is complicated by the absence of vibrationally-resolved features; in the absence of such features, vibrational hot bands and the possibility of large geometry changes upon photodetachment can obscure the vibrational origin of the transition between the anion and neutral electronic ground states. The arrows in Figs. 2 and 3 thus only reflect our best estimates of the cluster EAs. Determination of the error associated with the EAs is difficult, but we believe error bars of ± 0.10 eV for $x \leq 6$ and ± 0.15 eV for $x > 6$ to be reasonable.

Higher-resolution spectra of InP clusters containing less than nine atoms have been published previously and discussed elsewhere [18,19,27]. The spectra for these species presented here are in good agreement with the previous data. For these clusters the EAs stated in this Letter and the ones determined in the previous studies lie within ± 0.10 eV (see Table 1). The present spectra also confirm the assignment by Xu et al. [18] of a sharp feature observed at an eKE of ~ 2.9 eV in the 266 nm photoelectron spectra of the larger In_xP_y^- anions to a two-photon absorption process. These spectra were measured with a typical laser fluence of 70 mJ/cm^2 . The present study was performed with one-tenth the laser fluence, i.e., conditions less favorable for multi-photon processes. The sharp feature is absent in all the present spectra.

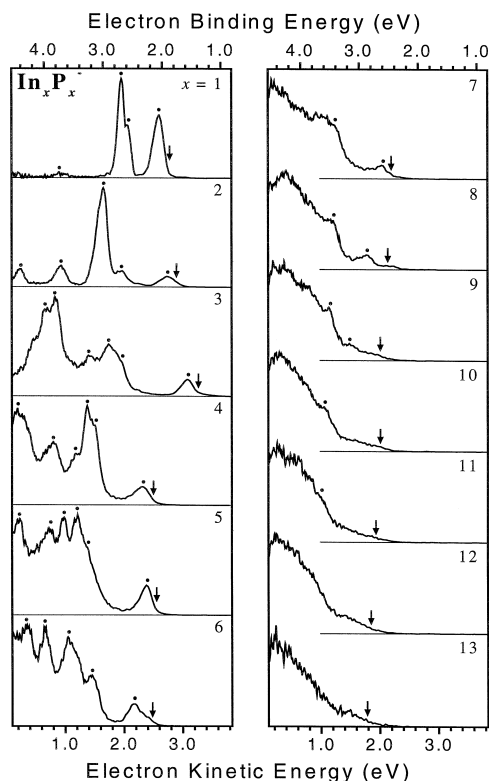


Fig. 2. 266 nm anion photoelectron spectra of stoichiometric indium phosphide clusters (In_xP_x^- , $x = 1-13$). Arrows indicate the estimated electron affinities. The vertical detachment energies of the bands marked with dots are listed in Table 1.

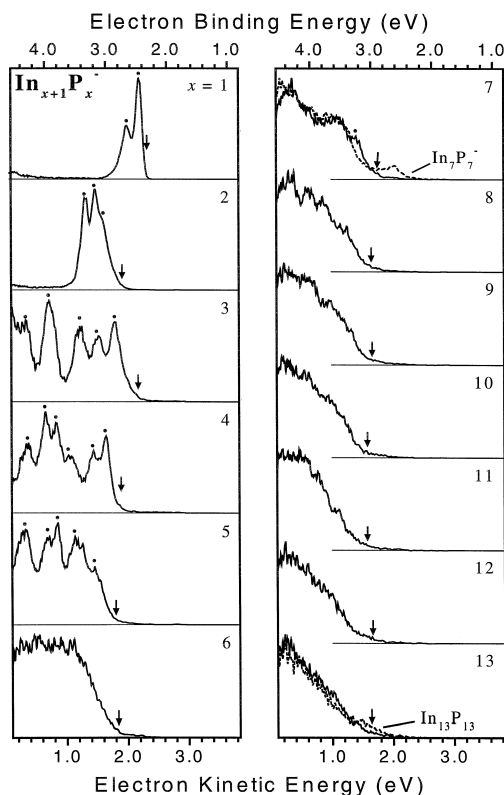


Fig. 3. 266 nm anion photoelectron spectra of non-stoichiometric indium phosphide clusters ($\text{In}_{x+1}\text{P}_x^-$, $x = 1$ –13). Arrows indicate the estimated electron affinities. The vertical detachment energies of the bands marked with dots are listed in Table 1. The dashed lines for $x = 7$ and $x = 13$ are the spectra of In_7P_7^- and $\text{In}_{13}\text{P}_{13}^-$ (see text).

The photoelectron spectra of the stoichiometric clusters In_xP_x^- (Fig. 2) show several interesting features. Distinct bands are observed up to $x = 6$, which we attribute to detachment transitions to the ground and low-lying electronic states of the neutral species. The isolated band at highest eKE in these spectra is assigned to the transition to the neutral electronic ground state. An abrupt change in the appearance of the photoelectron spectra is observed between $x = 6$ and $x = 7$. Instead of resolved bands, a broad, rather structureless feature now dominates the lower-eKE region. The center of this broad feature is gradually shifted to lower eKE with increasing cluster size. A weak band at high eKE can still be observed in the $x = 7$ spectrum. From $x = 7$ to $x = 9$ this weak band shifts to lower eKE, i.e., 2.04 eV ($x = 7$), 1.79 eV

($x = 8$), and 1.49 eV ($x = 9$). As a result of this, the signal onset for the $x \geq 8$ spectra does not correspond to the onset of a distinct band with an observable maximum, in contrast to the $x < 8$ spectra. Instead, the signal gradually increases without much structure from the signal onset. The only distinct feature that remains in the spectra of the larger clusters ($x = 10$ –13) is a considerable increase in slope of the signal ~ 0.5 –1 eV below the signal onset. Even though the appearance of the spectra of the stoichiometric clusters changes considerably with cluster size, the EA increases rather smoothly for $x > 4$ (see Table 1 and Fig. 5).

The photoelectron spectra of the non-stoichiometric $\text{In}_{x+1}\text{P}_x^-$ clusters are shown in Fig. 3. In contrast to the spectra of the stoichiometric clusters, an iso-

Table 1
Vertical detachment energies (VDEs) and electron affinities (EAs) of indium phosphide clusters (all energies are in eV)

Cluster	VDEs	EA ^a	EA ^{b,c}
InP	2.05, 2.60, 2.69, 3.75	1.88	1.95 ^b
In_2P	2.44, 2.63	2.33	2.400 ^c , 2.36 ^b
In_2P_2	1.98, 2.68, 3.00, 3.71, 4.40	1.75	1.68 ^b
In_3P_2	3.06, 3.19, 3.35	2.74	2.66 ^b
In_3P_3	1.57, 2.70, 2.91, 3.25, 3.82, 3.98	1.40	1.30 ^b
In_4P_3	2.86, 3.13, 3.43, 3.94, 4.32	2.48	2.43 ^b
In_4P_4	2.34, 3.15, 3.28, 3.47, 3.85, 4.46	2.15	2.07 ^b
In_5P_4	3.01, 3.22, 3.62, 3.82, 4.00, 4.28	2.76	
In_5P_5	2.27, 3.28, 3.44, 3.67, 3.93, 4.42	2.10	
In_6P_5	3.20, 3.52, 3.80, 3.94, 4.33	2.85	
In_6P_6	2.49, 3.20, 3.61, 4.00, 4.31	2.18	
In_7P_6		2.81	
In_7P_7	2.62, 3.42	2.45	
In_8P_7	3.26	2.86	
In_8P_8	2.87, 3.45	2.51	
In_9P_8		3.00	
In_9P_9	3.17, 3.52	2.65	
In_{10}P_9		2.99	
$\text{In}_{10}\text{P}_{10}$	3.59	2.65	
$\text{In}_{11}\text{P}_{10}$		3.06	
$\text{In}_{11}\text{P}_{11}$	3.68	2.72	
$\text{In}_{12}\text{P}_{11}$		3.08	
$\text{In}_{12}\text{P}_{12}$		2.80	
$\text{In}_{13}\text{P}_{12}$		2.99	
$\text{In}_{13}\text{P}_{13}$		2.87	
$\text{In}_{14}\text{P}_{13}$		3.03	

^aPresent study (± 0.1 eV for $x \leq 6$ and ± 0.15 eV for $x > 6$).

^bRef. [18] (± 0.05 eV).

^cRef. [19] (± 0.001 eV).

lated band at high eKE is not observed in the spectra of the $\text{In}_{x+1}\text{P}_x^-$ clusters. Consequently, the EA of a particular $\text{In}_{x+1}\text{P}_x$ cluster is higher than that of the corresponding In_xP_x (or $\text{In}_{x+1}\text{P}_{x+1}$) cluster. Up to $x = 5$ an increasing number of overlapping bands is observed in the lower-eKE region. Starting with $x = 6$ most of the structure observed in the spectra of the smaller clusters is replaced by a single broad feature at lower eKE. With increasing cluster size the slope of the signal decreases towards higher eKE. In contrast to the stoichiometric clusters, the EAs of the larger $\text{In}_{x+1}\text{P}_x$ clusters remain nearly constant (~ 3.0 eV). The spectra of the larger In_xP_x^- and $\text{In}_{x+1}\text{P}_x^-$ clusters also become more alike. This is indicated in Fig. 3 for $x = 7$ and $x = 13$. In the first case ($x = 7$), the two spectra are quite similar in the eKE region below 1.5 eV, but the In_7P_7^- spectrum shows an additional band at higher eKE. In the second case ($x = 13$), the additional band is not observed for the stoichiometric cluster and the spectra look rather similar. However, the EA of the odd cluster is slightly higher, and the increase in slope around 1.4 eV is more noticeable for the stoichiometric cluster.

In Fig. 4, the estimated EAs of the indium phosphide clusters In_xP_x and $\text{In}_{x+1}\text{P}_x$ ($x = 1\text{--}13$) are plotted as a function of cluster size. A clear oscillation in the EA is observed between the clusters containing an even and an odd number of atoms,

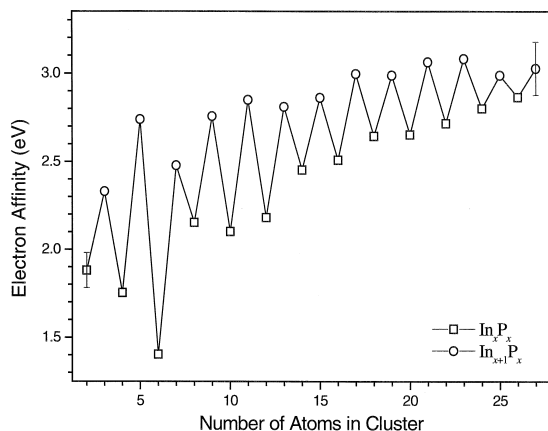


Fig. 4. Electron affinity of In_xP_x (open squares) and $\text{In}_{x+1}\text{P}_x$ clusters (open circles) as a function of cluster size. Solid lines are drawn only to guide the eye. Estimated error bars are ± 0.1 eV for $x \leq 6$ and ± 0.15 eV for $x > 6$.

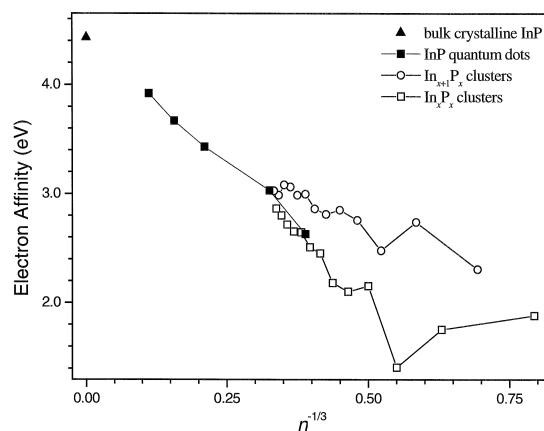


Fig. 5. Electron affinity of indium phosphide clusters as a function of $n^{-1/3}$, where n is the number of atoms in the cluster. Experimentally determined cluster electron affinities (open squares and circles), estimates of quantum dot electron affinities (solid squares, based on calculated conduction band minima in Ref. [5]) and the electron affinity of bulk crystalline InP (solid triangle, see text) are shown. Solid lines are drawn only to guide the eye.

with the odd numbered clusters having a considerably (up to 1.3 eV) higher EA. The difference in EA is largest for the smaller clusters and decreases with cluster size. In_3P_3 exhibits the smallest EA (1.40 eV) and largest ground state–excited state splitting (1.13 eV) of all the clusters studied. This indicates a particularly stable neutral species, in agreement with previous studies, which showed that relative to other InP clusters In_3P_3 is characterized by a high dissociation energy, large ionization potential and large abundance in the mass spectrum of InP clusters formed by laser ablation [20,21].

In Fig. 5 we compare results from the present study to the EA of InP quantum dots and bulk crystalline InP. For this comparison it proves useful to plot the EAs as a function of $n^{-1/3}$, where n refers to the number of atoms. $n^{1/3}$ is proportional to the effective diameter of an idealized crystalline-like cluster containing n atoms. The EA of crystalline InP (4.43 eV, solid triangle) was obtained from the known bulk ionization energy IE (5.85 eV) [28] and bulk band gap ΔE_g (1.42 eV) [29] using $\text{EA} = \text{IE} - \Delta E_g$. We also include results from Fu and Zunger [5], who have performed semi-empirical calculations on InP quantum dots of various sizes. These calculations reproduce the experimentally observed quan-

tum size effects on the band gaps of InP dots in the 700–9000 atom range [3,30,31]. EAs can be estimated (solid squares) from these calculations by the location of the conduction band minima (Fig. 9b in Ref. [5]) relative to the vacuum level. The two smallest calculated sizes overlap the size range probed in our experiments.

Our EAs for the larger clusters (open squares and circles in Fig. 5), in particular the stoichiometric clusters, show approximately the same size dependence as the theoretical EAs of the InP quantum dots. Moreover, we find good agreement between the theoretical EAs for 17 and 29 atom dots with our values for In_9P_9 and $\text{In}_{14}\text{P}_{13}$. A linear, least-squares fit to our EAs for the larger stoichiometric clusters ($x \geq 4$) yields an extrapolated bulk EA ($n \rightarrow \infty$) of 4.9 eV. This value lies within 0.4 eV of the experimentally derived value.

4. Discussion

The oscillatory pattern observed when plotting the EA as a function of cluster size (Fig. 4) reflects the open-shell/closed-shell alteration between clusters differing by a single atom (with an uneven number of electrons). This behavior has been noted in related photoelectron spectroscopy studies on III–V semiconductor cluster anions (GaP and GaAs) [14,17]. A similar alternation is seen in the electric polarizability of GaAs clusters [32]. In the stoichiometric In_xP_x clusters, photodetachment from the anion, which contains an odd number of electrons, results in a neutral cluster with an even number of electrons. The situation is reversed for the $\text{In}_{x+1}\text{P}_x$ clusters. The lower EAs for the stoichiometric clusters suggest that the neutrals are closed-shell species, whereas the higher EAs for the $\text{In}_{x+1}\text{P}_x$ clusters are consistent with open-shell neutrals and closed-shell anions.

The difference in the appearance of the photoelectron spectra of the even-numbered (stoichiometric) In_xP_x^- and the odd-numbered (non-stoichiometric) $\text{In}_{x+1}\text{P}_x^-$ cluster for the smaller clusters ($x \leq \sim 8$) has a similar origin. The spectra of the stoichiometric clusters show an isolated band at high eKE, which is absent in the spectra of the $\text{In}_{x+1}\text{P}_x^-$ clusters. The isolated band reflects the closed-shell na-

ture of the electronic ground state of the neutral In_xP_x clusters. A closed-shell system is generally characterized by a larger HOMO–LUMO gap than a comparable open-shell system, resulting in a larger energy difference between the electronic ground and first excited states. From the VDEs in Table 1, the gap between the ground and first excited states of the In_xP_x clusters up to $x = 7$ lies between 0.55 eV (InP) to 1.13 eV (In_3P_3). This gap is not apparent for the larger stoichiometric clusters. For the $\text{In}_{x+1}\text{P}_x$ clusters up to $x = 5$ the splitting between the two lowest electronic states is considerably smaller, ranging from 0.13 eV (In_3P_2) to 0.32 eV (In_6P_5).

A comparison of the current results to the absorption spectra of neutral InP clusters of Rinnen et al. [21] yields additional information on the nature of the electronic structure. Rinnen et al. performed resonant two-color and one-color photodissociation spectroscopy on neutral InP clusters, including In_3P_3 to In_7P_7 and In_4P_3 to In_7P_6 . The estimated absorption onset energies for the stoichiometric clusters In_3P_3 to In_7P_7 were 1.8, 1.4, 1.1, 1.0, and < 0.8 eV, respectively. 0.8 eV was the lower limit of the absorption measurements for In_7P_7 . For $x = 3$ and 4, these values are considerably higher than the gap between the ground and first excited states as seen in the anion photoelectron spectra. As discussed previously [18] this verifies that the first excited state in the photoelectron spectra is a low-lying triplet state. Transitions to these triplet states are not seen in the photodissociation experiment, because they are not optically allowed. The absorption onsets agree better with the gap in the photoelectron spectra for the larger clusters, indicating a decrease in the singlet–triplet splitting in the first excited state with cluster size.

The abrupt disappearance of most of the band structure in the In_xP_x^- and $\text{In}_{x+1}\text{P}_x^-$ photoelectron spectra with more than six In atoms is of interest. Such an effect could arise if the density of electronic states increased considerably, or if there were multiple isomers for the larger clusters, each with slightly different electronic structure. The existence of multiple isomers is well established for carbon and silicon clusters through ion mobility measurements [33,34]; similar experiments on InP clusters combined with ab initio calculations would be of considerable help in interpreting this trend in the photoelectron spectra.

Finally, we consider the experimental and calculated EAs in Fig. 5 in more detail. The quantum dots in the calculations of Fu and Zunger [5] are assumed to have the bulk crystalline structure of InP; a fictitious pseudopotential is added to simulate ‘passivation’ of the cluster, i.e., to eliminate low-lying states due to dangling bonds at the surface of the cluster. As a result, the electronic wavefunctions corresponding to the valence band maximum and conduction band minimum are largely delocalized within the quantum dot. In contrast, almost all of the atoms comprising the gas-phase clusters examined in the present study are located on or close to the cluster ‘surface’, due to the small number of atoms present in these clusters. Consequently, these atoms will rearrange in order to minimize the number of dangling bonds, resulting in a non-crystalline structure. The agreement between the experimental EAs and those obtained from the calculations is therefore quite remarkable. There are certainly errors in our estimated EAs, and the EAs obtained from the energy of the CBM alone do not account for charging of the quantum dots [35]. Nonetheless, the plot in Fig. 5 suggests a stronger connection than one might expect between the highest occupied molecular orbital in the bare cluster anions and the conduction band minimum in small passivated quantum dots, at least for stoichiometric clusters with more than 12 atoms. Alternatively, the electron affinities of the stoichiometric clusters may be relatively insensitive to the detailed bonding arrangement of the atoms and instead depend mainly on the total number of atoms.

This raises the issue of whether the clusters in the size range investigated here are beginning to exhibit ‘bulk’ or at least nanocrystalline properties. To investigate this further, it will be necessary to measure the photoelectron spectra at higher photon energies of the species studied here as well as larger InP cluster anions. Such experiments, planned for the near future, will indicate whether there is a ‘band gap’ in these clusters that extrapolates to the nanocrystalline and bulk values.

Acknowledgements

This research is supported by the National Science Foundation under Grant No. DMR-9814677.

KRA gratefully acknowledges a postdoctoral fellowship from the Swiss National Science Foundation.

References

- [1] A. Katz (Ed.), *Indium Phosphide and Related Materials: Processing, Technology and Devices*, Artech House, Norwood, MA, 1992.
- [2] O.I. Micic, C.J. Curtis, K.M. Jones, J.R. Sprague, A.J. Nozik, *J. Phys. Chem.* 98 (1994) 4966.
- [3] O.I. Micic, H.M. Cheong, H. Fu, A. Zunger, J.R. Sprague, A. Mascarenhas, A.J. Nozik, *J. Chem. Phys.* 101 (1997) 4904.
- [4] U. Banin, G. Cerullo, A.A. Guzelian, C.J. Bardeen, A.P. Alivisatos, C.V. Shank, *Phys. Rev. B* 55 (1997) 7059.
- [5] H. Fu, A. Zunger, *Phys. Rev. B* 55 (1997) 1642.
- [6] A. Tomasulo, M.V. Ramakrishna, *J. Chem. Phys.* 105 (1996) 3612.
- [7] O. Cheshnovsky, S.H. Yang, C.L. Pettiette, M.J. Craycraft, Y. Liu, R.E. Smalley, *Chem. Phys. Lett.* 138 (1987) 119.
- [8] T.N. Kitsopoulos, C.J. Chick, A. Weaver, D.M. Neumark, *J. Chem. Phys.* 93 (1990) 6108.
- [9] C. Xu, T.R. Taylor, G.R. Burton, D.M. Neumark, *J. Chem. Phys.* 108 (1998) 1395.
- [10] G.R. Burton, C. Xu, C.C. Arnold, D.M. Neumark, *J. Chem. Phys.* 104 (1996) 2757.
- [11] V.D. Moravec, S.A. Klopčic, C.C. Jarrold, *J. Chem. Phys.* 110 (1999) 5079.
- [12] S. O’Brien, Y. Liu, Q. Zhang, J.R. Heath, F.K. Tittel, R.F. Curl, R.E. Smalley, *J. Chem. Phys.* 84 (1986) 4074.
- [13] Y. Liu, Q.L. Zhang, F.K. Tittel, R.F. Curl, R.E. Smalley, *J. Chem. Phys.* 85 (1986) 7434.
- [14] C. Jin, K.J. Taylor, J. Conceicao, R.E. Smalley, *Chem. Phys. Lett.* 175 (1990) 17.
- [15] A. Nakajima, T. Taguwa, K. Nakao, M. Gomei, R. Kishi, S. Iwata, K. Kaya, *J. Chem. Phys.* 103 (1995) 2050.
- [16] L.S. Wang, H.B. Wu, S.R. Desai, J.W. Fan, S.D. Colson, *J. Phys. Chem.* 100 (1996) 8697.
- [17] T.R. Taylor, K.R. Asmis, C. Xu, D.M. Neumark, *Chem. Phys. Lett.* 297 (1998) 133.
- [18] C. Xu, E. Debeer, D.W. Arnold, C.C. Arnold, D.M. Neumark, *J. Chem. Phys.* 101 (1994) 5406.
- [19] C.C. Arnold, D.M. Neumark, *Can. J. Phys.* 72 (1994) 1322.
- [20] K.D. Kolenbrander, M.L. Mandich, *J. Chem. Phys.* 92 (1990) 4759.
- [21] K.-D. Rinnen, K.D. Kolenbrander, A.M. DeSantolo, M.L. Mandich, *J. Chem. Phys.* 96 (1992) 4088.
- [22] K.R. Asmis, T.R. Taylor, D.M. Neumark, *Chem. Phys. Lett.* 295 (1998) 75.
- [23] K.R. Asmis, T.R. Taylor, D.M. Neumark, *Eur. Phys. J. D* (1999, in press).
- [24] T.R. Taylor, K.R. Asmis, H. Gomez, D.M. Neumark, *Eur. Phys. J. D* (1999, in press).

- [25] R.B. Metz, A. Weaver, S.E. Bradforth, T.N. Kitsopoulos, D.M. Neumark, *J. Phys. Chem.* 94 (1990) 1377.
- [26] C. Xu, G.R. Burton, T.R. Taylor, D.M. Neumark, *J. Chem. Phys.* 107 (1997) 3428.
- [27] P.Y. Feng, K. Balasubramanian, *Chem. Phys. Lett.* 264 (1997) 449.
- [28] J. van Laar, A. Huijser, T.L. van Rooy, *J. Vac. Sci. Technol.* 14 (1977) 894.
- [29] H. Mathieu, Y. Chen, J. Camassel, J. Allegre, D.S. Robertson, *Phys. Rev. B* 32 (1985) 4042.
- [30] O.I. Micic, J.R. Sprague, C.J. Curtis, K.M. Jones, J.L. March, A.J. Nozik, H. Giessen, B. Fluegel, G. Mohs, N. Peyghambarian, *J. Phys. Chem.* 99 (1995) 7754.
- [31] O.I. Micic, J. Sprague, Z. Li, A.J. Nozik, *Appl. Phys. Lett.* 68 (1996) 3150.
- [32] S. Schlecht, R. Schafer, J. Woenckhaus, J.A. Becker, *Chem. Phys. Lett.* 246 (1995) 315.
- [33] G. von Helden, P.R. Kemper, N.G. Gotts, M.T. Bowers, *Science* 259 (1993) 1300.
- [34] M.F. Jarrold, *J. Phys. Chem.* 99 (1995) 11.
- [35] L.E. Brus, *J. Chem. Phys.* 79 (1983) 5566.